J. Membrane Biol. 108, 197–205 (1989)

The Journal of
Membrane Biology

Characterization of Sodium and Pyruvate Interactions of the Two Carrier Systems Specific of Mono- and Di- or Tricarboxylic Acids by Renal Brush-Border Membrane Vesicles

Raymond Mengual, Marie-Hélène Claude-Schlageter, Jean-Claude Poiree, Micael Yagello, and Pierre Sudaka

Laboratoire de Biochimie, Faculté de Médecine, F06034 Nice Cedex, France

Summary. The experiments reported in this paper aim at characterizing the carboxylic acid transport, the interactions of pyruvate and citrate with their transport sites and specificity. The study of these carriers was performed using isotopic solutes for the influx measurements in brush-border membrane vesicles under zero *trans* conditions where the membrane potential was abolished with KCl preloading with valinomycin or equilibrium exchange conditions and $\Delta\psi = 0$.

Under zero *trans* condition and $\Delta\psi = 0$, the influence of pyruvate concentrations on its initial rates of transport revealed the existence of two families of pyruvate transport sites, one with a high affinity for pyruvate (K_t = 88 μM) and a low affinity for sodium (K_t = 57.7 mM) (site I), the second one with a low affinity for pyruvate (K_t = 6.1 mM) and a high affinity for sodium (K_t = 23.9 mM) (site II). The coupling factor [Na]/[pyruvate] stoichiometry were determined at 0.25 mM and 8 mM pyruvate and estimated at 1.8 for site I, and 3 when the first and the second sites transport simultaneously.

Under chemical equilibrium ($\Delta\psi \simeq 0$) single isotopic labeling, transport kinetics of pyruvate carrier systems have shown a double interaction of pyruvate with the transporter; the sodium/pyruvate stoichiometry also expressed according to a Hill plot representation was n = 1.7. The direct method of measuring Na^+/pyruvate stoichiometry from double labeling kinetics and isotopic exchange, for a time course, gives a n = 1.67.

Studies of transport specificity, indicate that the absence of inhibition of lactate transport by citrate and the existence of competitive inhibition of lactate and citrate transports by pyruvate leads to the conclusion that the low pyruvate affinity site can be attributed to the citrate carrier (tricarboxylate) and the high pyruvate affinity site to the lactate carrier (monocarboxylate).

Key Words sodium · pyruvate · transport · proximal tubule · kinetics · kidney

Introduction

The Na^+-dependent monocarboxylic acid transporter, specifically the one for lactate, has recently been characterized [1, 3, 5, 7, 18, 20, 21] as well as its transport mechanism [10, 11]. It has been demonstrated that the monocarboxylic acid transporter was rather chemically specific. When a single carboxylic group was present, a higher ability was shown for molecules with 3 to 6 carbons [14]. In rabbit kidney brush borders, citrate or ketoglutarate were carried by a Na^+-dependent transport system [9, 18, 21], which can also transport succinate [24]. It has been shown that the dicarboxylate transport system deals with molecules with a basic structure of a non-ramified carboxylate in a *trans* configuration, the carbon of which can be substituted by small steric groups [20].

Moreover, it should be noted that the sodium coupling (stoichiometry) of the tricarboxylates is 2 to 3 whereas that of the monocarboxylates (lactate) is a maximum of 2 in the kidney brush border [10, 11] and 1 in the intestinal brush border for the same solute [5]. From microelectrode studies, in the presence of Na^+ gradient, a coupling factor of 3 sodium ions for the transport of completely dissociated di- and tricarboxylates has also been suggested [16].

The transport of monocarboxylic acids, or di- and tricarboxylic acids on the other hand, would appear to depend on different families of transporters [23]. However, the structure of the transported solutes poses a problem about the occurrence of intermediate sites common to both families of transorters.

The aim of this study was to determine in plasma membrane vesicles from renal cortex [12] the presence or absence of the overlapping of the carboxylate carrier specifications, namely between the monocarboxylic and di- or tricarboxylic carrier systems. We have observed the high specificity of these last two systems using pyruvate, which is carried by a two-site system corresponding to the lactate and citrate carriers.

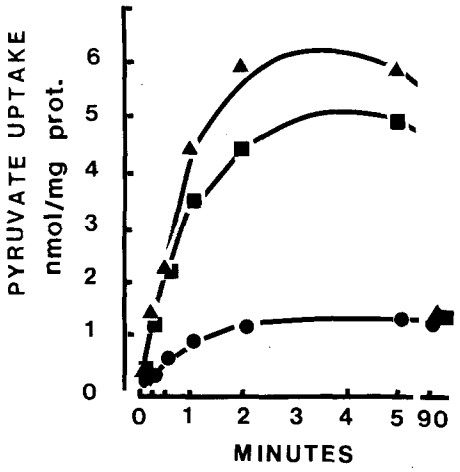

Fig. 1. Effect of Na or K gradients on the time course of pyruvate uptake in renal brush-border vesicles. All experiments were carried out under iso-osmolarity maintained with mannitol (300 mOsm) and buffered conditions (10 mM HEPES-Tris, pH 7.4). The NaCl and KCl salt concentrations were adjusted to iso-osmolarity with choline chloride. All uptake measurements were obtained at 20°C using rapid filtration techniques through nitrocellulose filters. [^{14}C] pyruvate (1 mM) uptake by vesicles was measured over 90 min. For the indicated extravesicular salt concentrations, KCl or NaCl was mixed with the transport buffer containing labeled pyruvate. For the indicated intravesicular salt concentrations, vesicles were pre-equilibrated in solution containing these salts. Uptake under electrochemical Na gradient (■) ($[Na]_{in}$ = 10 mM, $[Na]_{out}$ = 100 mM, $[K]_{in}$ = $[K]_{out}$ = 10 mM). Uptake under electrochemical Na gradient *increased* by a diffusion potential (▲), $[K]_{in}$ = 100 mM, ($[Na]_{in}$ = 10 mM, $[Na]_{out}$ = 100 mM, $[K]_{out}$ = 10 mM). Uptake in presence of choline-chloride gradient (out) 100 mM, $[K]_{in}$ = 10 mM (●). (Number of experiments = 3.) All experiments were performed in presence of valinomycin (10 μg/mg membrane protein)

Materials and Methods

Whole cortex from horse kidney was cut in slices 2 millimeters thick [15]. The pyruvate uptake experiments using [^{14}C] pyruvate were studied by a rapid mixing and filtration technique through nitrocellulose filters (Sartorius 0.65 μm). All experimental conditions are specified in the legend of each figure. Incubations were stopped using an ice-cold stop solution (buffered by HEPES[1]-Tris 10 mM) of choline chloride (100 mM) and KCl (50 mM). In all experiments, membrane vesicles were preloaded with valinomycin (10 μg/ml of membrane protein). Results reported in this paper are from three to five vesicle preparations, each point being in triplicate.

Pyruvic acid in solution was obtained from Fluka (Buchs-Switzerland); L-lactic acid (water solution) from SERVA (Heidelberg, Germany); all other chemicals were obtained from Sigma (St. Louis, MO); and [1,5-^{14}C]-citric acid (15 mCi/mmol), [L-U-^{14}C] lactic acid (100 mCi/mmol) and [U-^{14}C] pyruvic acid (12 mCi/mmol) were from Amersham France Corporation (Paris).

[1] HEPES: N-2 hydroxyethyl piperazine N'-2 ethanesulfonic acid.

Table 1. Effect of cations on initial rates of pyruvate transport

Salt	Percent of initial rates of pyruvate influx
KCl	100
NaCl	142 ± 16
NaSCN	518 ± 22
RbCl	80 ± 12
LiCl	92 ± 10
CsCl	85 ± 14
Chol Chl	86 ± 16

Membrane vesicles in 300 mM mannitol and 10 mM HEPES-Tris, pH 7.4, were incubated with 1 mM [^{14}C] pyruvate and various 100-mM salt gradients (measured at 3 sec) at 20°C. The initial rate of uptake of ^{14}C pyruvate in the presence of KCl gradient was taken as reference 100 and had the value of 1.85 ± 0.23 nmol/min × mg protein. These results are the means ± SE for triplicate samples and three membrane preparations.

Results

Driving Forces and Cation Specificity of Pyruvate Transport

The effect of various ionic gradients on the pyruvate uptake was studied in the presence of valinomycin (10 μg/mg membrane protein). As shown in Fig. 1, the uptake of 1-mM pyruvate was strongly activated when an electrochemical sodium gradient was imposed upon the intravesicular medium from the incubation medium. When an additional diffusion potential was applied with an electrochemical sodium gradient (100 mM), preloading membrane vesicles with 100-mM KCl, a higher accumulation of the pyruvate was observed. This uptake, which was higher than the equilibrium value, indicated an accumulation against its concentration gradient for the first 3 min of incubation. These results also demonstrated a membrane potential sensitivity of the pyruvate uptake.

A choline-chloride gradient did not lead to the same activating effect and no overshoot was observed. The sodium specificity for the Na^+-pyruvate cotransport appears from this time course. The relative effect of various salts on pyruvate transport is summarized in Table 1 with a reference value for the pyruvate uptake at 5 sec in the presence of an outer KCl gradient (100 mM); no significant difference was noted between the cations tested, i.e., K, Pb, Li, Cs or choline. But as previously demonstrated, the sodium was stimulating the pyruvate uptake and moreover when the anion of this sodium salt was the thiocyanate (SCN). This property demonstrates that the rapid diffusion of the SCN anion

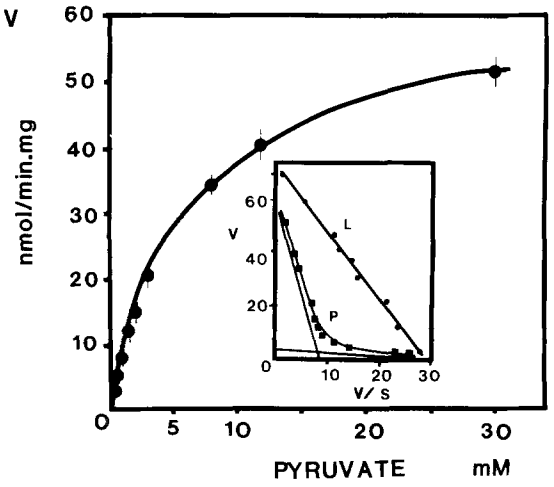

Fig. 2. Velocity curve of pyruvate transport. Vesicles were preloaded with 50 mM KCl, 200 mM mannitol and 10 mM HEPES-Tris, pH 7.4, in the presence of valinomycin (10 μg/mg protein). The incubation medium contained 50 mM KCl, 100 mM NaCl and 0.1 to 30 mM [^{14}C] pyruvate. Each value was corrected for the Na-independent pyruvate uptake obtained with 100 mM choline chloride. Inset: Woolf-Augustinsson-Hofstee representation v *vs.* $v/[S]$ of the same data (P = pyruvate). The ^{14}C lactate transport tested in the same conditions as pyruvate, i.e., 0.1 to 35 mM (L = lactate). The single diffusion flux was subtracted. (The incubation time was 3 sec)

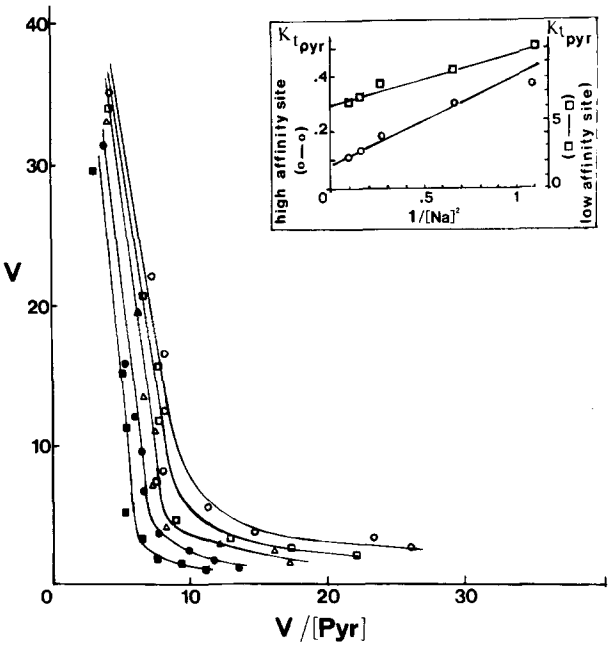

Fig. 3. Influence of pyruvate concentrations on its influx velocities for various sodium concentrations. Woolf-Augustinsson-Hofstee representation, v *vs.* v/[pyruvate]. Initial velocities of [^{14}C] pyruvate influx were measured after 3 sec (incubation time) under sodium and pyruvate chemical gradient. Vesicles were preloaded with 50 mM KCl, 200 mM mannitol and 10 mM HEPES-Tris, pH 7.4, in the presence of valinomycin (10 μg/mg protein). The incubation medium contained 50 mM KCl, 0.1 to 8 mM of [^{14}C] pyruvate and 30 mM (■), 40 mM (●), 60 mM (△), 80 mM (□) or 100 mM (○) NaCl. Each value was corrected for the Na-independent pyruvate uptake observed with choline chloride. v is expressed in nmol/min · mg protein; v/[pyruvate] in nmol/mM · min · mg protein. Inset: sodium effect on pyruvate K_t: $K_{t_{pyr}}$ (mM) *vs.* 1/[Na]^2 (10^{-3} × mM^{-2}). K_t values were obtained by a computer program, which made a linear regression of the velocity curve for enzyme showing two families of active sites. The high affinity site K_t varies from 0.1 up to 0.4 mM pyruvate (○); the low affinity site K_t varies up to 10 mM pyruvate (□—□)

increases the inner electronegative membrane potential activating the pyruvate uptake and consequently the electrogenic nature of the Na-pyruvate cotransport.

Kinetics of Pyruvate Flux

The kinetics of pyruvate flux were studied under the following pyruvate and sodium conditions: Zero *trans* conditions where $[\text{pyruvate}]_{in} = [\text{Na}]_{in} = 0$ and $\Delta\psi \simeq 0$, and equilibrium exchange conditions, i.e., $[\text{pyruvate}]_{out} = [\text{pyruvate}]_{in}$ and $[\text{Na}]_{out} = [\text{Na}]_{in}$ and $\Delta\psi \simeq 0$.

Influence of Pyruvate Concentration on Its Influx Rate (Zero Trans Conditions and $\Delta\psi \simeq 0$)

In the presence of 100-mM choline chloride or KCl, a single diffusion process of the pyruvate uptake was found where $v = 1.70$ nmol/min × mg protein × mM.

Figure 2 illustrates [Na], the effect of pyruvate concentration on its velocity uptake for 100 mM. Even if the system transport appears saturable near 30 mM pyruvate, we can observe on the inset a curvilinear Eadie Hofstee plot suggesting a multiple transport pathway for pyruvate as shown by Nord et al. [13]. The [^{14}C]-lactate transport has shown in the same conditions only one family of transport site in the range of concentrations tested (inset Fig. 2). By computer analysis of these experimental points, we have estimated the linear equation corresponding to v *vs.* v/[S] for each pair of branch. The mathematical method used to fit data involved a least squares analysis of chemical equation of the hyperbola v *vs.* v/[S], which describes a transport process where two independent carriers transport the same substrate. These respective lines in the inset of Fig. 2 for the pyruvate (P) represent the two Michaelis-Menten components obtained after resolution of curvilinear plots.

This analysis was applied when various sodium concentrations were tested giving a series of biphasic curves (Fig. 3). This result remains in agreement

Table 2. Kinetic parameters of sodium pyruvate cotransport (under sodium and pyruvate gradient conditions)

	High affinity site	Low affinity site
$K_{t_{pyr}}$	88 ± 12 μM	6.1 ± 0.580 mM
K_t Na	57.7 ± 3.1 mM	23.9 ± 2.5 mM
V_m	3.68 ± 0.51	60 ± 2.54 mM
k_{pyr}	0.0693 ± 0.010	0.0163 ± 0.0008

(V_m: nmol/min · mg protein; $k = V_m/K_t = min^{-1}$)

with the existence of two families of pyruvate transporters, one with an affinity site, the second with a low affinity site. Kinetic parameters are shown in Table 2.

We observed that sodium affects pyruvate affinity expressed by the constant of affinity $K_{t_{pyr}}$ from the slopes of biphasic curves (Fig. 3) and also reported in the inset of Fig. 3 (ordinate axis).

By linear regression, the actual linear plotting of each branch from these biphasic curves was deduced and a common maximal velocity observed (V_m, Table 2) for all Na^+ concentrations tested, when [Pyr] was saturating. Plotting the different $K_{t_{app\,pyr}}$ values *vs.* $1/[Na]^n$ concentration (Fig. 3 inset), a good linearity was obtained for $n = 2$ (correlation coefficient = 0.98). If we assume from this common V_m that this two-site system of pyruvate transport follows an ordered mechanism of Na and pyruvate binding as does the lactate transports [11] and glucose [6], we can apply this equation to this representation [11]:

$$K_{t_{pyr\,app}} = K_{t_{pyr}} K_{t_{Na}} 1/[Na]^2 + K_{t_{pyr}} \quad (1)$$

giving on the y axis the $K_{t_{pyr}}$ and $1/K_{t_{Na}}$ on the x axis.

The apparent pyruvate (K_t) affinity constant at each site was used to calculate the pyruvate affinities, respectively ($K_{t_{pyr}}$ by extrapolation), at infinite sodium concentrations. By extrapolation, the values recorded in the inset of Fig. 3 give the pyruvate affinities (on the ordinate axis) at the two sites as 88 μM ± 12 and 6.1 ± 0.58 mM.

The rate constant (first order k_1) for the high affinity family was about six times that of the low affinity one, demonstrating a high specificity of the high affinity site (site I) for the pyruvate uptake.

Moreover, if we consider that 2 is the mean number of Na^+ ions interacting with the carrier system, we can also determine the $K_{t_{Na}}$ ions by graphical extrapolation (inset Fig. 3) on the abcissa axis; the sodium affinities of the two families of site are 57.7 ± 3.1 mM and 23.9 ± 2.5 mM for the high and low affinity pyruvate sites, respectively. Thus, it appears that the high affinity pyruvate site has, on one hand, a sodium affinity ($K_{t_{Na}}$) about two times lower than in the case of the low affinity pyruvate site and, on the other hand, a V_m about 15 times lower (368 *vs.* 60 nmol/min · mg protein).

Influence of Na Concentration on Pyruvate Influx (Zero Trans Condition and $\Delta\psi \simeq 0$)

The Eadie-Scatchard equation [19] was applied to study the Na effect on pyruvate transport and the substrate was the sodium in this case: $v/[Na]^n$ *vs.* v for two pyruvate concentrations (0.25 and 8 mM). If the pyruvate carrier is a two-site system, we can assume that the high affinity site is mainly efficient at 0.25-mM pyruvate. Figure 4*a* shows that when $n = 2$ these data are fitted by a straight line. On the abscissa axis $V_{m_{app}}$ is 4.4 nmol/min × mg. Figure 4*a* was used to determine precisely the coupling factor at the peak of the Eadie-Scatchard plot [19] ($v/[Na]$ *vs.* v) $n = 1/1 - V'$ where $v' = v/V_m$ and the v value corresponding to the peak, we found $n = 1.80$.

From the slope of the linear plotting (Fig. 4*a*), we can also deduce $K_{t_{Na}}$ if we assume that these Na sites are equivalent; the $K_{t_{Na\,app}} = 35$ mM.

At 8 mM pyruvate, where the two sites are loaded by the pyruvate (Fig. 4*b*), the coupling factor found is $n = 3$, as well as from the graphical representations giving a linear plotting ($V_{m_{app}} = 36.5$ nmol/mg × min) then from the peak of the Eadie-Scatchard plot (v/Na *vs.* v) ($n = 2.9$); and then if we assume that Na interactions are equivalent, the $K_{t_{Na_{app}}}$ is 19 mM. Thus, at 8 mM pyruvate, the increase of the coupling factor (Na/Pyr) and the sodium affinity can be attributed to the second transport site from these data. We observed (Table 3) that, for the range of pyruvate concentrations applied, the $K_{t_{Na\,app}}$ of the high affinity pyruvate site, is nearly double that of the low affinity pyruvate site and was efficient for higher concentrations as previously observed; moreover, the two different coupling factors for these two pyruvate sites could characterize two pyruvate transport sites.

Influence of Pyruvate Concentration on Its Flux Rate (Equilibrium Exchange Conditions $[Pyr]_{in} = [Pyr]_{out}$ and $[Na]_{in} = [Na]_{out}$, $\Delta\psi \simeq 0$)

Two studies, one by single labeling (using [^{14}C] pyruvate) and the other by double labeling (using [^{14}C] pyruvate and ^{22}Na), were applied to characterize pyruvate transport in the absence of membrane potential.

Single Labeling Study: Membrane vesicles preloaded with various pyruvate and sodium (or choline) chloride concentrations and with 50 mM KCl

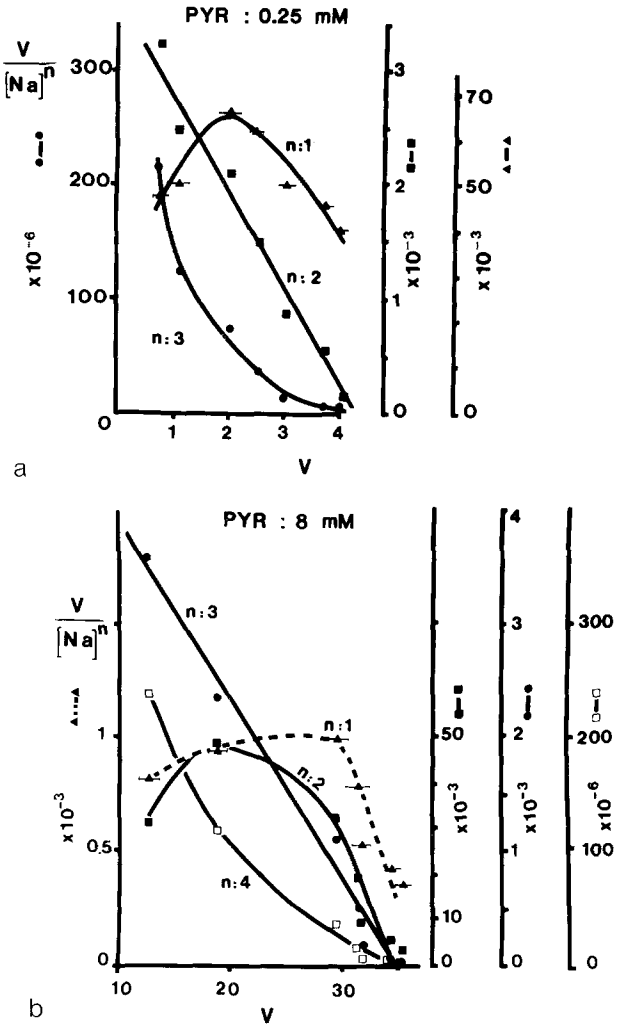

Fig. 4. Influence of Na concentration on pyruvate influx, $v/[Na]^n$ *vs.* v representation. The sodium gradients were from 15, 20, 30, 40, 60, 80 to 100 mM. Up to 80 mM, the sodium concentration was replaced by choline chloride to obtain 100 mM of the chloride salt. The incubation medium contained 50 mM KCl. Vesicles were preloaded with 50 mM KCl, 200 mM mannitol and 109 mM HEPES-Tris, pH 7.4, in the presence of valinomycin (10 μg/mg protein). (*a*) The uptake starts by addition of the incubation medium (previously described) containing 0.25 mM pyruvate. The incubation time was 3 sec. (*b*) Same experiment as in (*a*) where the pyruvate concentration was 8 mM. v is expressed as nmol/min · mg protein

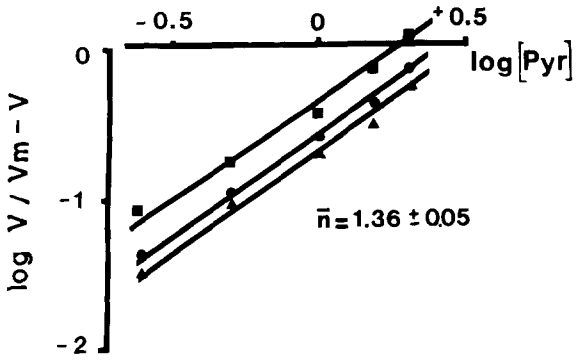

Fig. 5. Influence of pyruvate concentration on its influx rate (isotopic exchange). Hill plot representation log $v/V_m - V$ *vs.* log [pyruvate]. The inside and outside concentration mediums were the same except that the [^{14}C] pyruvate (0.25 to 4 mM) was in the outer vesicular medium. The sodium concentrations tested were 30 mM (■), 40 mM (●) and 100 mM (▲). (V_m used was obtained on the $1/v$ *vs.* 1/(pyr) plotting)

and 10 μM valinomycin/mg protein, were used to determine the initial rates of pyruvate isotopic exchange. These rates were measured by adding only an aliquot (10 μl) of [^{14}C]-pyruvate (at the same concentration as that of the preloading vesicles medium). After 3 sec of incubation, each sample was filtered as previously described. Hill plots of isotopic exchange kinetics are represented in Fig. 5.

The Hill number value is 1.36 ± 0.05 calculated from different Na^+ concentrations. These results indicate a multiple interaction of the pyruvate during the transport event. Another fitting of these data, the Eadie Scatchard representation (*not shown*), gave a parabolic curve (v/[pyr] *vs.* v) proving the existence of the two interdependent sites characterized by a cooperative mechanism between multiple substrate binding sites. From the Hill representation as a function of [Na] (*data not shown*), sodium/pyruvate stoichiometry is greater than one ($n = 1.7 \pm 0.07$); this coupling ratio, obtained at the chemical equilibrium of Na^+ and pyruvate, could be considered as a mean value if the two types of sites are differently coupled to the Na activation.

Double Labeling Study: These experiments were performed to determine the degree of coupling of the two cotransported solutes at chemical equilibrium using their isotopes, ^{22}Na and [^{14}C] pyruvates, simultaneously.

As in the lactate experiments [10], Na-pyruvate cotransport was measured in the presence of 20-mM ^{22}Na and 5-mM [^{14}C] pyruvate. Control measurements of the uptake of one solute without the other enable the interdependence of the two solutes absorption to be determined. The results from the simultaneous uptake at 3.5, 12, 25, 40 and 60 sec are summarized in Fig. 6. The uptake percentages of the two solutes in relation to equilibrium, expressed as $1 - F$ (F = nmol at time t/nmol at equilibrium) are correlated: [^{14}C] pyruvate against ^{22}Na on logarithmic scales. The slope of 1.67 shows the Na-pyruvate cotransport coupling factor to be higher than 1 (under equilibrium conditions of the two solutes).

These results confirmed by isotopic exchange of [^{14}C] pyruvate, could demonstrate that Na effect is an activation of positive cooperatively or a multi-

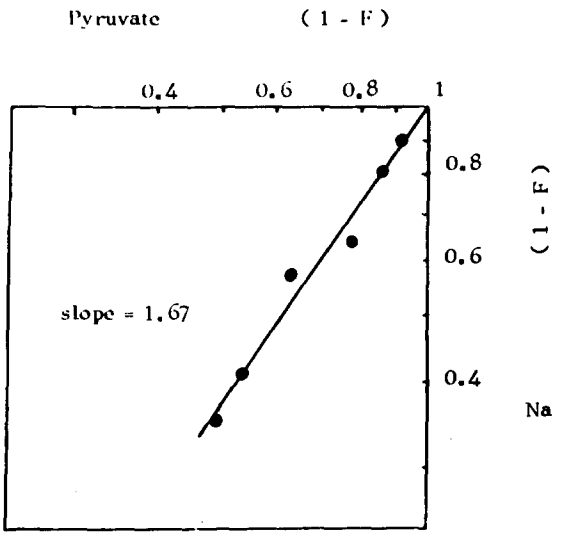

Fig. 6. Correlation between ^{22}Na and [^{14}C] pyruvate uptakes under chemical equilibrium of the two solutes (log-log scale representation). These data were obtained using the same time course for isotopic Na and pyruvate uptakes at 3, 5, 12, 25, 40 and 60 sec; the uptake compared to equilibrium is expressed as $(1 - F)$. F is the ratio of uptake value at one incubation time *vs.* the uptake at equilibrium (90 min). The sodium-independent [^{14}C] pyruvate uptake and pyruvate-independent Na uptake were subtracted from the data.

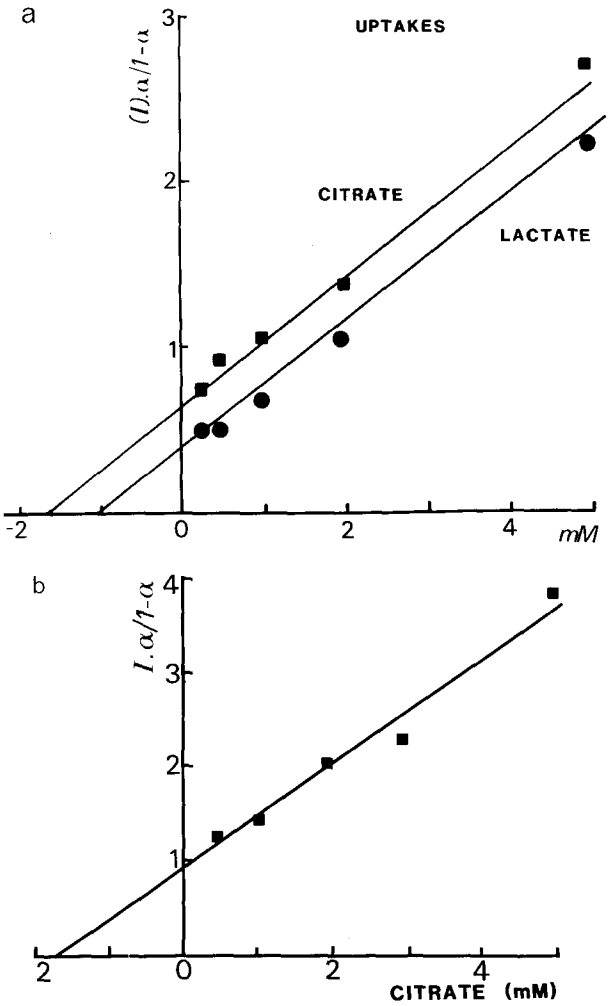

Fig. 7. Pyruvate influence on the L-lactate and citrate transport. Hunter and Down representation: $[I] \times \alpha/(1 - \alpha)$ *vs.* (concentration of transported solute) both expressed in nM, $[I]$; inhibitor concentration, i.e., 1 mM pyruvate in this case; $\alpha = V_i/V_o$, V_o = control velocity and V_i = velocity in the presence of I. Incubation conditions were 100 mM NaCl or choline chloride, 50 mM KCl, 10 mM HEPES-Tris, pH 7.4, and isotopic solute [^{14}C] citrate or L-[^{14}C] lactate. Membrane vesicles were preloaded with 50 mM KCl, 200 mM mannitol, 10 mM HEPES-Tris and valinomycin (10 μg/mg of membrane protein). Initial rates were taken at 3 sec by rapid filtration on cellulose nitrate membranes as described in Materials and Methods. The stop and washing solution was 100 mM choline chloride, 50 mM KCl, 10 mM HEPES-Tris, pH 7.4. (*a*) [^{14}C] lactate and [^{14}C] citrate transport for a range of substrate concentrations indicated in abscissa in the presence of 1 mM pyruvate in the incubation medium. (*b*) [^{14}C] citrate transport in the presence of 18 mM L-lactate and 1 mM pyruvate in the incubation medium. All data obtained in the presence of Na are corrected for the simple diffusion measured in the absence of Na (replaced by choline chloride)

site activation [17]. Since, however, a direct measurement of the coupling factor (by double labeling of ^{22}Na and [^{14}C] pyruvate uptake) gives a number of 1.67 Na ions per pyruvate molecule, as observed at saturating pyruvate concentrations, we assume that Na^+ has at least two types of interaction considered as a multiple essential activation.

Specificity of Each Pyruvate Transport Site

Since pyruvate is transported by two families of transporters and it was suggested [25] that the two transporter types were those for lactate (monocarboxylic) and citrate (polycarboxylic), it seemed important to determine the overlapping of the transporter specifications in our system and the type of competition occurring between the solutes during transport.

Inhibition of the Lactate and Citrate Uptakes by Pyruvate

The initial rates of the sodium-dependent L-[^{14}C] lactate transport were measured at 0.25- and 5-mM lactate concentrations. Inhibition by 1 mM citrate was practically null (1.2 ± 0.3% and 0.5 ± 0.2% for 0.25-mM and 5-mM lactate, respectively).

Figure 7*a* shows the effect of 1 mM pyruvate on the lactate or citrate uptake (abscissa values) where

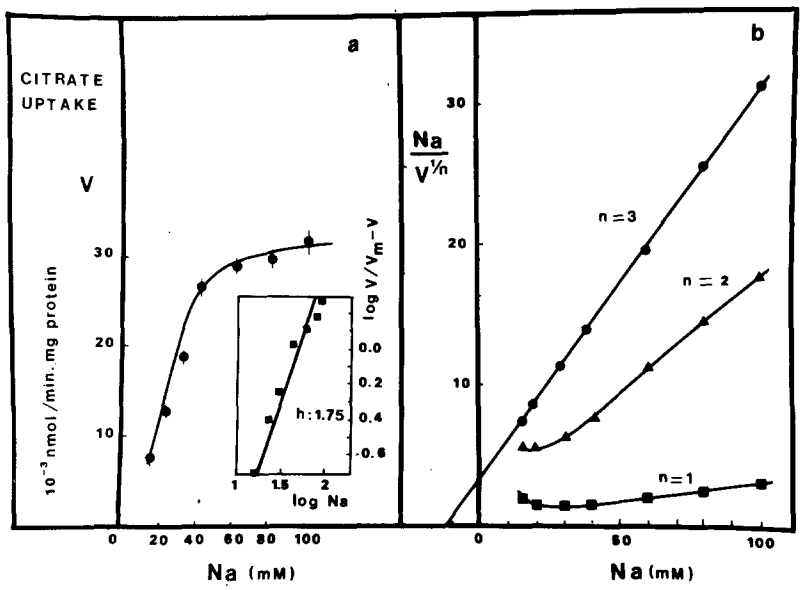

Fig. 8. Influence of sodium on initial rates of [^{14}C] citrate. (*a*) The effect of Na concentrations were examined in the presence of [^{14}C] citrate, 0.5 mM and 50 mM KCl, 10 mM HEPES-Tris, pH 7.4; choline chloride was used to maintain iso-osmolarity at 300 mOsM. Before incubation, membrane vesicles were preloaded with 200 mM mannitol, 50 mM KCl and valinomycine (10 μg/mg protein). The incubation time was 3 sec and filtration conditions were the same as in Fig. 6. Inset: Hill representation of the same data, i.e., log v ($V_m - v$) *vs.* log [Na]. V_m (33.10^{-3} nmol/min × mg protein) (maximum velocity) used in this representation was obtained from a reciprocal plot of the data. (*b*) Garay and Garrahan representation $Na/V^{1/n}$ *vs.* [Na] from the Fig. 8*a*. For a value of $n = 3$, a good linearization was obtained (assuming that these three sodium sites are identical)

the inhibition is expressed as the product of [*I*] inhibitor concentration by the activity ratio (ordinate value) as defined by Hunter and Downs [2] equations:

$$[I] \cdot \frac{\alpha}{1-\alpha} = K_i + \frac{K_i}{K_m} \cdot [S] \qquad (2)$$

where $\alpha = V_i/V_o$ activity coefficient ratio, V_i inhibition velocity and V_o control velocity.

Inhibition by 1 mM pyruvate indicates a competitive type since linearization of the results is an increasing function of the lactate concentration (in noncompetitive inhibition this ratio would be concentration independent). From this representation, the K_i of pyruvate (0.400 ± 0.038 mM) and the K_t of lactate (1 mM) is determined.

[^{14}C] citrate transport was inhibited by pyruvate (1 mM), under the same experimental conditions as for the L-lactate experiments (Fig. 7*b*). The pyruvate-citrate transporter interaction is also one of competitive inhibition. The K_m of citrate (1.7 mM) is, like that of lactate, higher than the K_i pyruvate, (0.64 ± 0.05 mM).

These results confirm that the pyruvate substrate is transported by two transporters, those of lactate and of citrate, which are distinct since citrate does not affect lactate transport (Table 3).

Table 3. Kinetic parameters of Na interaction on pyruvate transport

Pyruvate	0.25 mM	8 mM
$K_{t_{app}}$ Na	35 mM	19 mM
n coupling factor:		
Linear fitting	2	3
Peak value	1.83	2.9

Sodium Dependent of the Citrate Transporter

We have measured the degree of coupling of sodium with the citrate transporter, and its affinity, in order to complete the comparative study of the lactate, pyruvate and citrate transport sites. The effect of sodium on citrate transport is shown in Fig. 8. We have developed two models to analyze the Na activation for the citrate uptake as applied to succinate [3]. The data shown in Fig. 8*a* (transport rate *vs.* Na concentration), were also analyzed by the Garay and Garrahan representation $[Na]/v^{1/n}$ *vs.* [Na]) [4, 22]. As shown in Fig. 8*b*, the best value giving a linear transformation is obtained only when $n = 3$, assuming that 3 sodium ions interact on multiple binding sites and have an identical affinity. The $K_{t_{app}}$ Na, determined on the abscissa axis is 13 ± 2.1 mM for a 0.5-mM citrate concentration and the $V_{m_{app}}$, estimated from the slope, is 43.5 nmol/min × mg. This last value of $V_{m_{app}}$ for the same citrate concentration is used for our second analysis to fit the logarithmic representation of the Hill equation (inset Fig. 8*a*); this plotting yielded a Hill coefficient of 1.75 for this range of Na^+ concentrations. This Hill coefficient assumes the cooperative effect of each sodium interaction on the transport system site. The K' value (intercept plot) is estimated at 683.

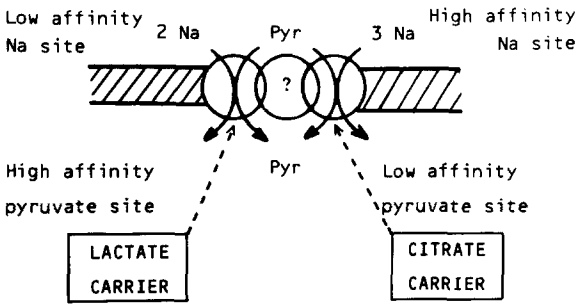

Fig. 9. Schema of the two transport pyruvate sites. The lactate carrier (left) and the citrate carrier (right)

Discussion

Our experimental results suggest several conclusions: (i) The main driving force permitting the transmembrane passage of pyruvate is the chemical sodium gradient. (ii) Pyruvate is transported by two families of sites for which the pyruvate and sodium affinities are different as the coupling factor of Na with pyruvate. (iii) The fact that pyruvate inhibits the lactate and citrate transporters, but that citrate does not inhibit the lactate transporter, suggests that the first family of sites (site I) corresponds to the lactate transporter and the second to that of the citrate. The distinction between these two sites is proposed from the kinetic parameters.

Thus, the main data in this paper corresponds to the existence of a multiple pyruvate interaction with the carrier system. This conclusion is suggested from the transport studies under chemical gradient conditions and at the chemical equilibrium. The chemical gradient shows two independent transport sites.

The data obtained by isotopic exchange of [^{14}C]-pyruvate (Hill plot) confirm the suggestion that the interaction of more than one pyruvate ion reacts with its transportation system.

Indeed the data from the above analyses separately, concerning lactate and citrate transport, suggest that site I (high affinity) and site II (low affinity) for the pyruvate transport should be assigned to the specific transporters of lactate and citrate, respectively.

In the case of the high affinity site I, the parameters $K_{t_{Na}}$, k are similar to those obtained for lactate transport [11]. Inhibition kinetics, however, have shown that pyruvate has a higher affinity (expressed by $K_{i_{pyr}} = 0.4$ mM) than lactate on site I measured for [^{14}C] lactate transport. The difference in the maximum rate (V_m) could correspond either to a modification of the number of sites available on the external face of the membrane or to reduction of the translocation rate constant. It should be noted, however, that the low value for the maximum rate does not affect the efficiency of the transporter, k (V_m/K_t), which is similar for the lactate and pyruvate transports (site I). The sodium affinities of the two transporter types are different. This, and the lactate coupling coefficient are additional evidences that site I is the lactate transporter (the monocarboxylic acid carrier).

Site II shows similar $K_{t_{Na}}$ and V_m values for pyruvate or citrate transport: thus, neither the interaction with sodium $K_{t_{Na}}$ nor the maximum transport capacity (V_m) is modified. That the transporter has a lower efficiency (expressed by k) for pyruvate than citrate, confirms a higher specificity of site II for citrate than for pyruvate.

Competitive inhibition of citrate transport by pyruvate may be the result of either a mutual exclusion of the two solutes or an interaction of each solute with different specific sites, assuming a common third site, which could be concerned with citrate transport. Competition at this site would result in mutual exclusion of pyruvate and citrate. The pyruvate K_i of 0.64 mM could be related to citrate transport by pyruvate $K_i = 0.95$ mM (in the presence of a saturating lactate concentration for its specific transporter) showing that pyruvate and citrate are mutually exclusive at the low affinity site.

In conclusion, our experiments demonstrate that the transport sites for monocarboxylic acids, such as lactate, and for tricarboxylic acids, such as citrate are district and are responsible for transport specificity (Fig. 9).

The present study of pyruvate transport, with accurate measurements of the kinetic parameters, furthers our existing knowledge [13, 14, 22].

The high specificity of the family of monocarboxylic acid transporters was demonstrated, and in the same family a slight variability in affinity depending either on the substitutions of carboxyl function [14] or on a modification of carboxyl function. It has also been shown that citrate transporter specificity extends to dicarboxylic acids such as succinate [14]. This double specificity of the citrate transporter would explain its capacity to interact with pyruvate. In this case, it would not be the α-hydroxyl group of the lactate but rather the ketone function, which would interact with the second carboxylic site with higher or lesser affinity according to whether the site had been initially activated by citrate (low K_i) or not (high K_m of pyruvate) at the low affinity level of the site. A chemical and specific labeling of these sites will allow more precisely definitions of these mechanisms.

These results, on whole cortex, complement the data recently published on the pyruvate trans-

port by rabbit proximal tubule and about the malate interaction on this system [8].

We thank Mrs. N. Limare for excellent technical assistance and Mrs. A. Rainaud and Mrs. H. Steiner for secretarial assistance.

References

1. Barac-Nieto, M., Murer, H., Kinne, R. 1980. Lactate-sodium cotransport in rat renal brush border membrane. *Am. J. Physiol.* **239:**F496–F506
2. Dixon, M., Webb, E.C. 1964. Enzymes. (2nd ed.) Academic, New York
3. Fritzsch, G., Haase, W., Rumrich, G., Fasold, H., Ullrich, K.J. 1984. A stopped flow capillary perfusion method to evaluate contraluminal transport parameters of methylsuccinate from interstitium into renal proximal tubules cells. *Pfluegers Arch.* **400:**250–256
4. Garay, R.P., Garrahan, P.J. 1973. The interactions of sodium and potassium with the sodium pump in red cells. *J. Physiol. (London)* **231:**297–325
5. Hildman, B., Storelli, C., Haase, W., Barac-Nieto, M., Murer, M. 1980. Sodium ion/L-lactate cotransport in rabbit small-intestinal brush border membrane vesicles. *Biochem. J.* **186:**169–176
6. Hopfer, U., Groseclose, R. 1980. The mechanism of Na^+-dependent D-glucose transport. *J. Biol. Chem.* **255:**4453–4462
7. Jorgensen, K.E., Sheikh, M.I. 1984. Renal transport of monocarboxylic acid. *Biochem. J.* **223:**803–807
8. Jorgensen, K.E., Sheikh, M.I. 1988. Transport of pyruvate by luminal membrane vesicles from pars convoluta and pars recta of rabbit proximal tubule. *Biochim. Biophys. Acta* **938:**345–352
9. Kippen, I., Hirayama, B., Klinenberg, J.R., Wright, E.M. 1979. Transport of tricarboxylic acid cycle intermediates by membrane vesicles from renal brush border. *Proc. Natl. Acad. Sci. USA* **76(7):**3397–3400
10. Mengual, R., Leblanc, G., Sudaka, P. 1983. The mechanism of Na^+L-lactate cotransport by brush border membrane vesicles from horse kidney. *J. Biol. Chem.* **288(24):**15071–15078
11. Mengual, R., Sudaka, P. 1983. The mechanism of Na^+-L-lactate cotransport by brush border membrane vesicles. *J. Membrane Biol.* **71:**163–171
12. Murer, M., Smaj, P. 1986. Transport studies in plasma membrane vesicles isolated from renal cortex. *Kidney Int.* **30:**171–186
13. Nord, E., Wright, S.H., Kippen, I., Wright, E.M. 1982. Pathways for carboxylic acid transport by rabbit renal brush border membrane vesicles. *Am. J. Physiol.* **243:**F456–F462
14. Nord, E.P., Wright, S.H., Kippen, I., Wright, E.M. 1983. Specificity of the Na^+-dependent monocarboxylic acid transport pathway in rabbit renal brush border membranes. *J. Membrane Biol.* **72:**213–221
15. Poiree, J.C., Vannier, C., Sudaka, P., Fehlmann, M. 1978. Glucose transport by horse kidney brush borders. I. Transport properties of brush border membrane closed vesicles. *Biochimie* **60:**645–651
16. Samarzija, I., Molnar, V., Frömter, E. 1981. The stoichiometry of Na^+ coupled anions absorption across the brush border membrane of rat renal proximal tubule. *In:* Advances in Physiological Sciences: Kidney and Body Fluids. L. Takacs, editor. Vol. 11, pp. 419–423. Pergamon, Oxford—New York—Sidney—Paris—Frankfurt
17. Segel, I.H. 1975. Enzyme Kinetics. pp. 1–945. John Wiley and Sons, New York
18. Sheridan, E., Rumrich, G., Ullrich, K.J. 1983. Reabsorption of dicarboxylic acids from the proximal convolution of rat kidney. *Pfluegers Arch.* **399:**18–28
19. Turner, R.J. 1983. Quantitative studies of cotransport systems: Models and vesicles. *J. Membrane Biol.* **76:**1–15
20. Ullrich, K.J., Fasold, H., Rumrich, G., Kloss, S. 1984. Secretion and contraluminal uptake of dicarboxylic acids in the proximal convolution of rat kidney. *Pfluegers Arch.* **400:**241–249
21. Ullrich, K.J., Rumrich, G., Kloss, S. 1982. Reabsorption of monocarboxylic acids in the proximal tubule of the rat kidney. *Pfluegers Arch.* **395:**212–219
22. Wright, S.H., Hirayama, B., Kaunitz, J.D., Kippen, I., Wright, E.M. 1983. Kinetics of sodium succinate cotransport across renal brush border membranes. *J. Biol. Chem.* **258:**5456–5462
23. Wright, S.H., Kippen, I., Klineberg, R.J., Wright, E.M. 1980. Specificity of transport system for tricarboxylic acid cycle intermediates in renal brush borders. *J. Membrane Biol.* **57:**73–82
24. Wright, S.H., Kippen, I., Wright, E.M. 1982. Stoichiometry of Na-Succinate cotransport in renal brush border membranes. *J. Biol. Chem.* **257:**1773–1778
25. Wright, S.H., Krasne, S., Kippen, I., Wright, E.M. 1981. Na^+-dependent transport of tricarboxylic acid cycle intermediates by renal brush border membrane: Effects on fluorescence of a potential sensitive cyanine dye. *Biochim. Biophys. Acta* **640:**767–778

Received 2 May 1988; revised 7 October 1988